Geochemistry International, Vol. 40, No. 8, 2002, pp. 723–738. Translated from Geokhimiya, No. 8, 2002, pp. 803–819.

Problems of the Stoichiometry and Thermobarometry of Magmatic Amphiboles: An Example of Hornblende from the Andesites of Bezymyannyi Volcano, Eastern Kamchatka

R. R. Al'meev*, A. A. Ariskin*, A. Yu. Ozerov, and N. N. Kononkova***

** Vernadsky Institute of Geochemistry and Analytical Chemistry, Russian Academy of Sciences, ul. Kosygina 19, Moscow, 119991 Russia*

*** Institute of Volcanology, Far East Division, Russian Academy of Sciences, bul'v. Piipa 9, Petropavlosk-Kamchatskii, 683006 Russia*

Received January 15, 2001

Abstract—The paper discusses the problem of the evaluation of Fe^{3+} and the calculation of the structural formula of natural and experimentally synthesized amphiboles. The currently used normalization schemes of amphibole analyses are demonstrated to commonly underestimate Fe_2O_3 and overestimate FeO. The data reported on the composition of hornblende from andesites of Bezymyannyi volcano are recalculated taking into account Mössbauer spectroscopic data. The hornblende composition is determined mostly by the edenitic and tschermakitic types of heterovalent substitution, which makes it possible to estimate the pressure (6–8 kbar) and temperature (800–920°C) during crystallization within the amphibole stability field. The plausibility of these estimates is tested in the context of the general problem of the use of magmatic Ca-amphibole for purposes of geothermobarometry.

INTRODUCTION

According to N. Bowen's reaction scheme [1], amphibole and biotite are the main water-bearing phases characterizing the closing stages of the fractional crystallization of mafic and intermediate magmas. This leads to the conclusion that amphibole plays an important part in the genesis of andesites and more silicic derivatives. However, this concept was questioned by Tilley, who pointed out the rarity of amphibole phenocrysts in lavas of the calc–alkaline series [2]. Later, the limited occurrence of amphibole in mafic and intermediate volcanic rocks was explained as resulting from phase decomposition under low pressures [3]. However, after the publication of experimental evidence [4], the presence of variably preserved hornblende grains was regarded as one of the typomorphic features of andesites. Starting from the 1960s, the fractionation of amphibole, a mineral characterized by a higher Fe/Mg ratio than those of olivine and pyroxenes, was utilized by some researchers in the interpretations of the petrochemical and geochemical trends of calc-alkaline rocks of island-arc and continental-margin volcanic series [5–9], granite and granodiorite magmatic complexes [10]. Experimental results [11] allowed the estimation of the stability field of hornblende in water-saturated basaltic magma and lay the basis of, first, the systematic experimental study of phase equilibria in natural basalts in water-bearing environments and, second, specialized investigations into the stability of amphibole at the liquidus of basalts and andesites (see the review in [12, 13]).

In the 1980s and 1990s, amphibole fractionation attracted closer attention as an important evolutionary factor of calc-alkaline magmas during intermediate and closing stages, mainly because of the relatively high amphibole–melt partition coefficients of several trace elements (including HREE, HFSE, and others) [14]. This made it possible to explain some features of the geochemical trends of some minor elements in the calc-alkaline series [9, 15–17]. It is worth mentioning that interpretations of these trends are usually made based on the results of simple mass-balance calculations for fractionation [8, 9, 15–18]. For example, Thirlwall *et al.* [9] explain the low Er/Yb ratio and depletion in Ti of andesites of the low-Ca M series in Grenada Island, Lesser Antilles, by the fractionation of the high-pressure *Ol* + Al-*Aug* + Al-*Sp* + *Hbl* assemblage from the parental picritic melts.[1] However, this led to the assumption that there were much higher temperatures (>1100°C) and lower H_2O concentrations in the parental melts than those within the amphibole stability field on the liquidus of mafic magmas [12, 19]. The cause of these discrepancies is obvious: models based on mass-

[1] Symbols of minerals and end-members: *Ol* = olivine, *Aug* = augite, *Sp* = spinel, *Pl* = plagioclase, *Hbl* = hornblende, *An* = anorthite, *Ab* = albite, *Fo* = forsterite, *Ed* = edenite, Fe-*Ed* = ferroedenite, *Richt* = richterite, *Parg* = pargasite, Fe-*Parg* = ferropargasite, Ti-*Parg* = titanic pargasite, *Hast* = hastingsite, Mg-*Hast* = magnesiohastingsite, *Tr* = tremolite, *Act* = actinolite, Fe-*Act* = ferroactinolite, *Tsch* = tschermakite, Fe-*Tsch* = ferrotschermakite, Fe-*Hbl* = ferrous hornblende, Mg-*Hbl* = magnesian hornblende, *Qtz* = quartz, *Or* = potassic feldspar, *Bi* = biotite, *Sph* = titanite, *Mt* = magnetite, *Ilm* = ilmenite, *Liq* = melt.

balance calculations are not consistent with realistic phase diagrams, including the stability conditions of the mineral phases under variable P–T–f_{O_2}–a_{H_2O} parameters, compositions, and phase proportions [20].

The petrogenetic role of amphibole in island-arc magmatism is not restricted only to the effect of this mineral during the closing stages. A quite important fact is that this mineral, one of the main phases of metabasites (and, to a lesser degree, of metahyperbasites) of the subducted oceanic lithosphere serves as a water transporter (along with phlogopite, clinohumite, and hydrosilicates) to the mantle wedge region and, thus, is one of the factors in the genesis of primary island-arc magmas that controls their geochemical features [21]. At the same time, the partial melting of an amphibole and/or garnet-bearing residue is widely utilized in models for the origin of tonalite–trondhjemite–granodiorite rock associations [22 and others].

These considerations demonstrate the pressing need for, and significance of, the development of *models for phase equilibria with the participation of amphibole*. The currently available extensive information on hornblende–melt phase equilibria (we found 49 references in the INFOREX [23] and MELT [2] petrological data bases, which include 325 compositions of melts and minerals) covers temperature and pressure intervals of 600–1100°C and 1 atm–27 kbar. This representative collection of data makes it possible to bring forth the problem of developing a system of amphibole–melt geothermobarometers for the petrogenetically important region of compositions and conditions. Note that the aforementioned massif of data does not include experiments on determining the melt–amphibole partition coefficients for minor elements, which are usually carried out by "doping" the starting material with oxides of rare and trace elements.

Further progress in the geothermobarometry of phase equilibria with the participation of amphiboles (two minerals or minerals with melt) is complicated by the extreme compositional variability of this mineral. The crystal structure of amphibole comprises a series of cationic sites, which can be occupied by elements with various ionic radii and valences. The chemistry of amphibole includes all major components (except P_2O_5), and its variations are controlled by more than ten iso- and heterovalent substitution mechanisms [24]. The situation is even more complicated by the fact that the amphibole structure may include iron in different oxidation states, and the anion group contains OH, O, F, and Cl. The elucidation of these relations requires either additional analytical studies (by conventional chemical, SIMS, and SmX techniques [25]) or specialized methods making it possible to evaluate the concentrations of these components, because information of this kind usually cannot be retrieved from experiments on the melting–crystallization of rocks. The principal importance of such knowledge for the use of amphibole with geothermobarometric purposes can be illustrated by the data in [26], which demonstrate the effect of the O(F,Cl)/OH substitution in the anion group on the calculated activities of hornblende end members.

Another experimental problem is related to the achievement of equilibrium between chilled phases, including amphibole [12], particularly in experiments at low temperatures, when the melt fraction is insignificant and it is highly viscous. Moreover, significant analytical difficulties are caused by the small dimensions of amphibole crystals synthesized at temperatures below 800°C. For instance, Scaillet and Evans [27] were forced to recalculate their microprobe analyses, which represented a mixture of small hornblende crystals and chill glass. An analogous problem was faced by experimentalists dealing with the melting of the amphibole–plagioclase assemblage at T = 1000°C and P = 12 kbar with various initial sizes of the fractions of the starting materials [28]. An important conclusion made by these researchers is as follows: while equilibrium was achieved in crystallization experiments at an experiment duration of approximately 48 h, equilibrium in experiments on the melting of an *Pl* + *Hbl* starting mixture was achieved only in more than eight days when the size fractions were <3 μm and was not detected even in 36 days when the fractions were >5 μm.

Another problem is the poor knowledge of the thermodynamic mixing properties of Ca-amphibole end members[3] because of the low mixing enthalpies of components, which are commensurable with the accuracy of the calorimetric techniques employed [30].

It is pertinent to recall that the facts cited above, on the one hand, hamper the development of a full thermodynamic description of the whole spectrum of Ca-amphibole solid solution (with allowance for multisite exchange equilibria) and, on the other, are sometimes regarded as a warrant to limit the considerations to simplified models, which relate variations in the intensive parameters with the behavior of single components (Al_{tot}) [31, 32], cation redistribution within crystal–lattice sites (Na–$K^{[A]}$, Fe–$Mg^{[M1–M3]}$) [33, 34], or the participation of a few end members in complex exchange equilibria of several minerals [35–37].

The very first problem arising when hornblende is inspected with the use of microprobe analyses is the evaluation of Fe^{3+}/Fe_{tot} and the recalculation of the structural formula. This problem is of principal significance for amphiboles, because the [A] site of this mineral may remain vacant, which precludes the calcula-

[2] This databank on melt–mineral equilibrium was compiled by A.V. Girnis at the Institute of the Geology of Ore Deposits, Petrography, Mineralogy, and Geochemistry, Russian Academy of Sciences, girnis@igem.ru.

[3] According to the latest report of the Subcommittee on Amphibole of the International Mineralogical Association (IMA 1997), amphibole compositions are subdivided into four groups, including 71 end members [29]: Mg–Fe–Mn–Li amphiboles (19 end members), Ca-amphiboles (21 end members), Na–Ca-amphiboles (14 end members), and Na-amphiboles (17 end members).

tion of the Fe^{2+} fraction in compliance with the idealized structural formula, as is practiced, for example, in the case of spinel [38]. This hinders the development of correct models for the activities of amphibole components and questions the warranty of using calculated values (estimates) of the mole concentrations of Fe^{2+}, Fe^{3+}, and other cations. This paper presents a brief outline of the problem of calculating the Fe^{3+} for naturally occurring and experimentally synthesized Ca-amphiboles. Direct estimates of Fe^{3+}/Fe_{tot} were made for hornblende from the andesites of Bezymyannyi volcano, structural formulas of the mineral were calculated, and the compositional evolution of this mineral is discussed in terms of the main exchange substitutions. These data were further used as the empirical basis for the analysis of thermobarometric techniques in application to magmatic amphiboles (from calc–alkaline rocks).

AMPHIBOLE STRUCTURAL FORMULA AND THE ESTIMATION OF THE Fe^{3+} FRACTION

In order to analyze the compositional trends of the principal rock-forming minerals, mole fractions of their end members are usually employed (such as *An* in *Pl*, *Fo* in *Ol*, etc.). This simple approach leads to far from trivial problems in the case of amphibole, whose crystal chemistry permits cations to simultaneously occupy a number of structural positions (sites). At the same time, Ca-amphibole alone comprises 21 end members [29], and although the compositions of natural hornblendes can be quite accurately described by as few as nine or ten end members [37, 39], none of them seems to be able to adequately represent the integral evolution of the composition of this mineral. This definitely stems from the multicomponent chemistry of amphibole (it contains nearly all major components) and, perhaps, also the relatively narrow crystallization interval (as compared with other silicates), which predetermines fairly insignificant compositional variations. Because of this, in characterizing the compositional variations of amphibole, it is common to consider (1) the concentrations of cations per one formula unit in a given structural position (for example, $^{[IV]}Al$ and $^{[VI]}Al$) and (2) the substitution mechanisms of cations, including heterovalent (for example, the edenitic scheme, see below) and isovalent ($Fe^{2+} \Leftrightarrow Mg^{2+}$ and $^{[Al]}K \Leftrightarrow {}^{[A]}Na$). In both situations, it is necessary to calculate the structural formula of the amphibole (Fig. 1) on the basis of its microprobe analyses [40]. This, in turn, requires estimation of the proportions of Fe^{2+} and Fe^{3+}, which can vary over broad limits in amphiboles.

The compositions of natural amphiboles are recalculated in compliance with a variety of schemes with different chemical and stoichiometric limitations for the anhydrous basis (normalized to 23 oxygen atoms) [36, 41, 42]. For example, assuming that all iron occurs in the form of Fe^{2+} (the most frequently employed presupposition) or Fe^{3+}, the sum of cations is normalized to 13eCNK or 15eNK values.[4] In other instances, based on stoichiometric considerations, an average between the maximum and minimum permitted Fe^{3+} contents in the amphibole structure (the former virtually always corresponds to the 13eCNK scheme for Ca-amphiboles, while the latter means $Fe^{3+} = 0$ or the 15eNK scheme; Fig. 1). All of these calculation routines and their limitations are discussed in much detail in [40].[5] It is generally though that the 13eCNK scheme yields a good approximation of the Fe^{2+} and Fe^{3+} proportions for Ca-amphiboles, while 15eNK is more useful for Fe–Mg–Ca-amphiboles [45]. Blundy and Holland [46] note that a calculation making use of an average between 13eCNK and 15eNK reproduces the Fe^{3+} values of amphiboles yielded by conventional "wet" chemical techniques with errors of up to 28%, which also affects the estimated concentrations of cations in other sites. The errors in the estimation of cation concentrations increase therewith in the sequence T < (M1, M2, M3) < M4 < A [31]. According to Holland and Blundy [46], the error in the $^{[IV]}Al$ calculation is 3%, with the errors in the cation occupancy of [A] sometimes becoming as great as 20%. Because of this, in the general case, the [A] site is the most sensitive to analytical errors and the calculation scheme selected.

Based on full chemical analyses of metamorphic hornblendes (including the determination of their Fe^{3+}, OH, F, and Cl), Cosca *et al.* [26] tested different calculation procedures of amphibole structural formulas. It turned out that none of the techniques yielded satisfactory results, with the Fe_2O_3 contents always underestimated and FeO overestimated. The H_2O concentrations of the hornblendes exhibited no systematic correlations between the measured and calculated values, although the latter were usually higher (see Figs. 2–4 in [26]). Cosca *et al.* [26] established that H_2O estimates made on the basis of stoichiometric considerations do not correspond to the actual values, even if the F_2 and Cl_2 concentrations were measured on a microprobe.

Figure 2 compares the three calculation techniques of the amphibole structural formulas using the results on 30 Ca-amphiboles with known Fe^{2+} and Fe^{3+} proportions. Comparing different recalculation procedures, it can be concluded that the errors in Fe^{3+} by the 13eCNK technique are 27%, while the cation occupancies of

[4] 13eCNK means the normalizing of the cations to the $(13/\Sigma^{cations} - Ca - Na - K)$ value on the presumption that Fe^{2+}, Mg, and Mn do not occupy [M4]; 15eNK is a cation normalization to the $(15/\Sigma^{cations} - Na - K)$ value on the presumption that Na does not enter [M4].

[5] We recast the calculation scheme for the amphibole structural formula proposed in [43] as an MS EXCEL electronic table, with the structural-formula calculation including an additional procedure of the distribution of Fe^{2+} and Mg between the M2, M4, and M13 (joint) sites, according to [42, 44]. The user can select from a variety of calculation schemes proposed, and the *Hbl* compositions can be plotted in classification diagrams and plots of exchange equilibria (see below).

Amphibole structural formula

General amphibole formula $A_{0\text{-}1}B_2C_5^{VI}T_8^{IV}O_{22}(OH)_2$,
where ***A***, ***B***, ***C***, ***T***, and **OH** correspond to the following crystallographic sites (p.f.u.):

A	***A*** site (10- to 12-fold coordinated)	usually occupied by Na, <u>K</u>* or a vacancy
B	two 6- to 8-fold coordinated ***M4*** sites	Na, <u>Ca</u>, Mg, Fe^{2+}, Mn
C	five 2***M1***, 2***M2***, and 1***M3*** octahedral sites	Mg, Fe^{2+}, Mn, Al, <u>Fe^{3+}</u>, Ti
T	eight 4***T1*** and 4***T2*** octahedral sites	Al, <u>Si</u>
OH	two anionic sites	OH, F, Cl, O

Occupancy of sites in the amphibole structure and stoichiometric constrains

Site	Cation	Stoichiometric limits	Estimated proportions Fe^{3+} min	Fe^{3+} max	Note:
T	**Si****	**Si ≤ 8**	**8Si**		Much Si, all Al in ***C***
	Al	**ΣAl ≥ 8**		**8SiAl**	Al occupies ***T*** and ***C***
	Ti				
	Cr				
	Fe^{3+}				
C	**Mg**				
	Ni				
	Zn				
B	**Fe^{2+}**				
	Mn	**ΣMn ≥ 13**		**13eCNK**	Ca and Na in ***B***, Fe^{2+}, Mg, Mn in ***C***
	Ca	**ΣCa ≤ 15**	**15eNK**		Ca only in ***B***, Na only in ***A***
	Na	**ΣNa ≥ 15**		**13eK**	All Na in ***B***
A	**K**	**ΣK ≤ 16'**	**16CAT**		***A*** is not occupied
	□				

*Underlined symbols indicate that the cation can occupy only this site.
**Cations are listed in order of increasing ionic radii.

Fig. 1. Idealized amphibole formula, preferable occupancy of crystal chemical sites, and stoichiometric constraints, which make it possible to estimate the minimum and maximum Fe^{3+} contents (based on data from [40]). Legend: 8Si: the normalization coefficient is such that Si = 8; 8SiAl: the sum Si + Al = 8; 13eCNK (otherwise denoted as ΣMn ≥ 13): the sum of cations from Si to Mn inclusive = 13 (except Ca, Na, and K), etc.

other sites ($^{[VI]}$Al, $^{[M4]}$Na, $^{[A]}$Na, and mg#) remain at a minimum. The Al concentration at the octahedral site is always somewhat overestimated (by 5–11%), and the Mg mole fraction (mg#) and $^{[A]}$Na can be better calculated by the 13eCNK procedure.

For *experimentally synthesized amphibole*s, the aforementioned recalculation schemes can be used along with direct techniques that make use of the Fe^{3+}/Fe_{tot} of the amphiboles depending on the redox conditions of the experiments (Table 1).

For example, Ernst and Liu [45] recalculated analyses of amphiboles synthesized at the QFM buffer relying on the $Fe^{3+}/Fe_{tot} = 0.125$. Obviously, this approach is applicable only to conditions with a buffered oxygen fugacity (by the QFM, MH, or other buffers), when the iron redox state in the amphibole varies insignificantly with temperature, as is observed in melts [49] and rocks [50]. However, this does not hold for biotite and amphibole [51]. Popp *et al.* [51] conducted hydrothermal experiments on a sample of titanic pargasite from alkaline basalt at variable f_{O_2} and $500 < T < 1000$°C, 1 atm $< P <$ 10 kbar, and measured (by Mössbauer spectroscopy) Fe^{3+}/Fe_{tot} ratios. This enabled the researchers to determine that a nearly linear tempera-

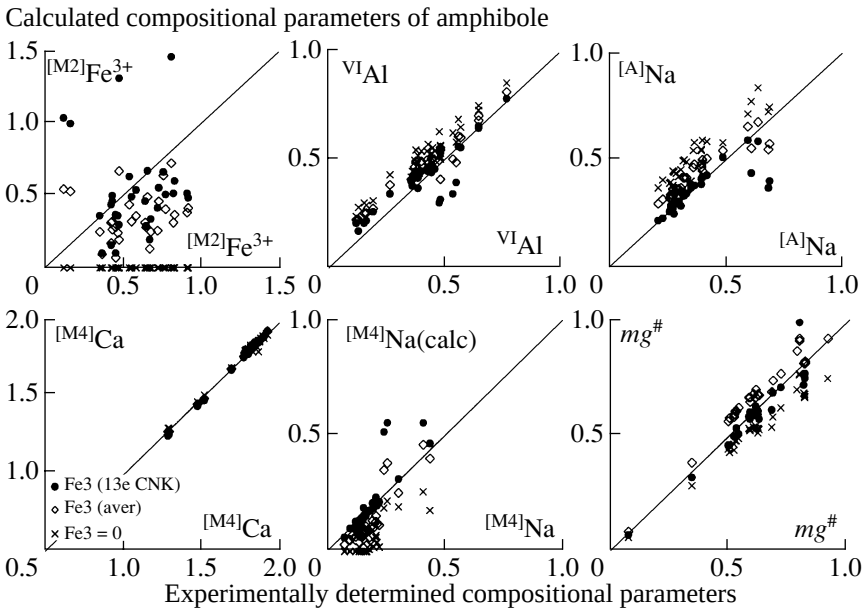

Fig. 2. Comparison of different calculation procedures of Fe^{3+}/Fe_{tot} in amphibole.

ture dependence of the Fe^{3+}/Fe_{tot} of the amphiboles is typical of all of the buffer equilibria (Fig. 3). These authors also noted that the dependence weakens with a decrease in the oxidation state—the slopes of the approximating lines systematically diminish with the transition from the MH to the NNO buffer, so that either no temperature dependence can be detected for the CCH4 buffer (over the interval of T = 700–1000°C) or this dependence changes its sign (at T = 500–700°C).

The problem of the estimation of the Fe^{3+}/Fe_{tot} was discussed in [25]. The authors of this paper mention that the oxygen pressure in nature is controlled by the chemistry of minerals and melts, while the experiments in [51] were carried out within the subsolidus region, where the synthesized amphibole occurred in equilibrium with a fluid phase but not a melt.

Using a new analytical technique for determining Fe^{2+} and Fe^{3+} in minerals and silicate glasses [52], King *et al.* [25] were the first to determine the Fe^{3+} and H^+ in a Ti-pargasite, which was synthesized in basanitic melt under pressures of 15–20 kbar at varying oxygen fugacities. An important result of this research was the establishment of the fact that the Fe^{3+}/Fe_{tot} of the coexisting equilibrium amphibole and melt were quite similar at four different oxygen buffers (Table 1). The Fe^{3+}/Fe_{tot} partition coefficient between the amphibole and melt was equal to one at the IW and MH buffers and did not exceed 1.1 under intermediate redox conditions (at the fayalite–ferrosilite–magnetite, FFM, and NNO buffers) [25]. This fact is important because it opens up the possibility of estimating the Fe^{2+} and Fe^{3+} proportions in experimentally synthesized amphiboles (earlier, a series of empirical dependences was proposed for estimating the Fe^{3+}/Fe_{tot} melts; see review [53]). However, this leaves uncertain as to whether this approach can be extended over (1) lower pressure conditions and (2) all Ca-amphiboles. The point is that the accent in [25] is placed on the development of a technique for the estimation of the redox state of mantle magmas. Experi-

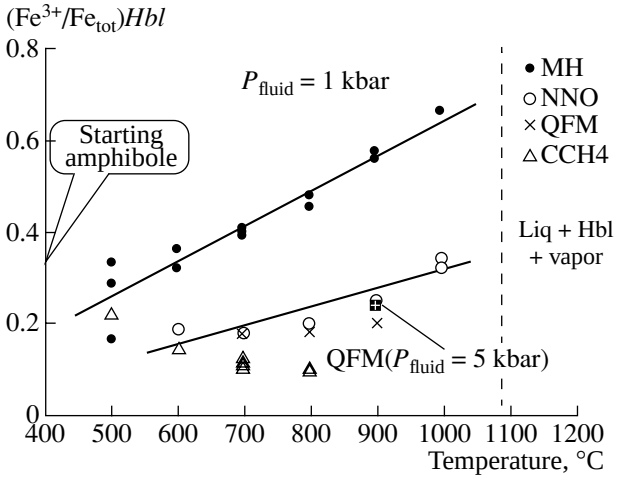

Fig. 3. Variations in Fe^{3+}/Fe_{tot} as functions of temperature at a pressure of 1 kbar. Experimental determination for a Ti-pargasite sample from the Vulcan's Throne alkaline basalt. Symbols correspond to experiments conducted along the hematite–magnetite (HM), nickel–bunsenite (NNO), quartz–fayalite–magnetite (QFM), and graphite–methane (CCH4) buffer lines. The Fe^{3+}/Fe_{tot} ratio of the starting sample was 0.32. Solid diamond corresponds to the experiment at 5 kbar, QFM. The analogous experiment at 10 kbar is indistinguishable from the experiment at 5 kbar (based on data from [48]).

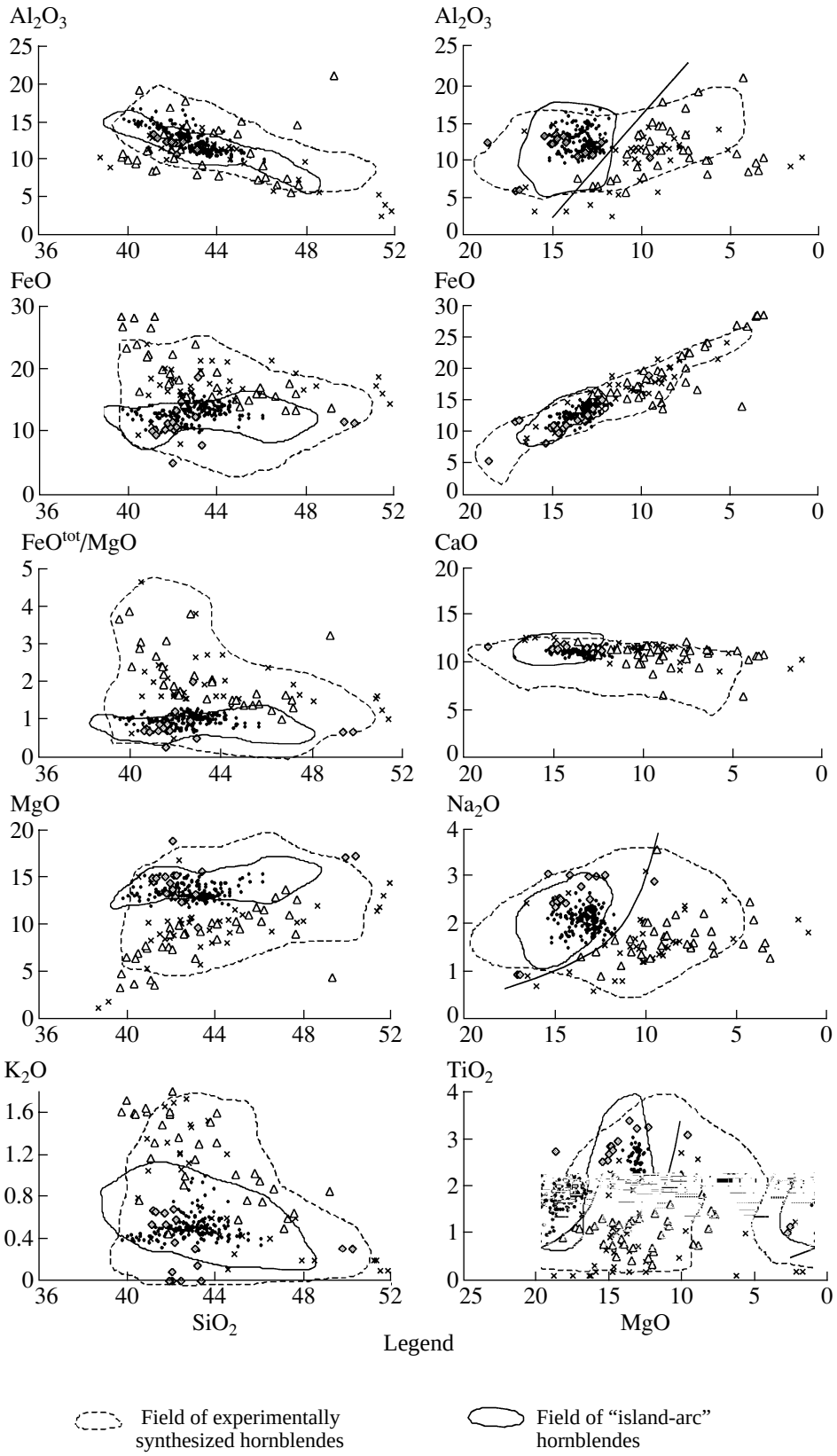

Fig. 4. Comparison of the compositions of hornblendes from different rock types: solid spots = hornblende from Bezymyannyi volcano; triangles = calc–alkaline granitoid plutons [31, 54–57]; diamonds = gabbroids [58–60]; crosses = metabasites [26, 61]. Fields show the compositions of experimentally synthesized amphiboles and hornblende from rocks of calc–alkaline volcanic series [8, 15, 17, 18, 59, 62].

Table 1. Direct measurements of the Fe^{3+}/Fe_{tot} in amphiboles experimentally synthesized under different redox conditions

Oxygen buffer	Fe^{3+}/Fe_{tot}	*T*, °C	*P*, kbar	Amphibole	Starting composition	Analytical technique	Reference
CCH4	0.15	650	1	*Hbl*		WCh	[47]
IW	0.16	1100	20	Ti–*Parg*	basanite	SmX	[25]
WM	0.11	700	1	*Hbl*	MORB	MS	[48]
NNO-2	0.12	1150/1092	15	Ti–*Parg*	basanite	SmX	[25]
QFM	0.13	700	1	*Hbl*	MORB	MS	[48]
QFM	0.18	650	1	*Hbl*		WCh	[47]
FFM	0.35	1200/1175	20	Ti–*Parg*	basanite	SmX	[25]
FFM	0.46	1200/1175	20	Ti–*Parg*	basanite	SmX	[25]
NNO	0.20	650	1	*Hbl*		WCh	[47]
MH	0.30	650	1	*Hbl*		WCh	[47]
MH	0.40	700	1	*Hbl*	MORB	MS	[48]
MH	0.65	1200/1175	20	*Hast*	basanite	SmX	[25]

Note: WCh is "wet" chemistry, MS is Mössbauer spectroscopy, SmX is synchrotron micro-X-ray absorption [25].

mentally synthesized Ti-pargasite (with 0.3–0.4 f.u. of Ti per 23 oxygens) in equilibrium with basanitic melt is compositionally close to kaersutite (Ti > 0.5), which, in contrast to other amphiboles, possesses an additional oxygen atom in its structural formula and is characterized by the predominance of Fe^{3+} over Fe^{2+}. Furthermore, it remains uncertain whether the dependences proposed for the estimation of the Fe^{3+}/Fe_{tot} ratios are applicable to the andesite–dacite region of melt compositions [53].

DISTINCTIVE COMPOSITIONAL FEATURES OF AMPHIBOLES FROM THE ANDESITES OF BEZYMYANNYI VOLCANO

In this section, data are presented on hornblende from the andesites of the 1956 directed explosive eruption. The samples were taken during joint fieldwork of the teams from the Vernadsky Institute of Geochemistry and Analytical Chemistry, Russian Academy of Sciences, and the Institute of Volcanology, Far East Division, Russian Academy of Sciences, in 1997. The chemistry of the minerals was analyzed at Vernadsky Institute on a CAMEBAX-MICROBEAM microprobe at a standard accelerating potential of 15 kV and a beam current of 30 nA. The diameter of the focused electron beam was 2 μm. We analyzed 150 hornblende crystals.

COMPARISON OF HORNBLENDE COMPOSITIONS

The variation diagrams in Fig. 4 demonstrate the field of experimentally synthesized amphiboles (from the INFOREX database) and the compositions of naturally occurring amphiboles in rocks of different types: (1) island-arc calc-alkaline basaltic andesites, andesites, and dacites (this field is outlined with a solid line), (2) plutonic calc-alkaline granitoids, (3) mafic ophiolitic gabbroids, and (4) metabasites. The compositions of hornblende from the 1956 eruption andesites fall into the field of "island-arc" amphiboles. As the silica content increases, their compositions show insignificant variations in CaO and the FeO/MgO ratio (with an average of 0.96), a decrease in Al_2O_3, and an increase in the CaO/Al_2O_3 ratio. The compositions of hornblende from gabbroids are restricted to the field of "island-arc" amphiboles but are higher in Na and Ti. This is consistent with the conclusion in [63], according to which there are no principal differences between the compositions of "intrusive" and "volcanic" amphiboles from parental rocks with 45–55% SiO_2. However, this review of amphiboles of magmatic origins contains no mention of compositions typical of calc-alkaline granitoid plutons. As can be readily seen in Fig. 4, these compositions cover the whole spectrum of "island-arc" amphiboles in terms of SiO_2 concentrations but are higher in Fe and K at lower concentrations of Mg and Ti and elevated FeO/MgO ratios. The differences in the compositions (mg#) of "island-arc" and granitoid amphiboles can be naturally explained by the differences between the compositions of the parental melts or their differentiation degrees. Hornblendes from granitoids crystallized at notably lower subsolidus temperatures. It is interesting to mention that the field of "granitoid" amphiboles (for example, in an Al_2O_3 vs. MgO diagram) includes practically all data points of experimentally synthesized hornblendes in equilibrium with quartz. The fields of metamorphic amphiboles are also close to the compositions of "granitoid" hornblendes.

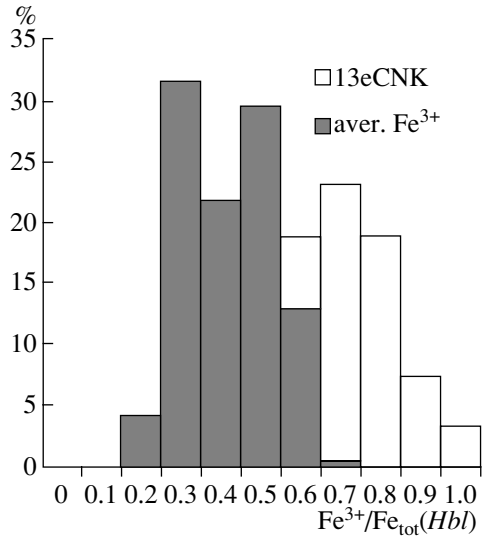

Fig. 5. Histogram of the distribution of Fe^{3+}/Fe_{tot} values of the examined hornblendes.

ESTIMATION OF Fe^{3+}/Fe_{tot} IN HORNBLENDE

In order to evaluate the oxidation degree of Fe, Fe^{3+}/Fe_{tot}, hornblende from andesites of Bezymyannyi volcano were inspected with the aid of Mössbauer spectroscopy [64]. The material for analysis was obtained by the subsequent magnetic separation, separation in bromoform, and handpicking under a binocular magnifier of large (2–1 and 1–0.5 mm) size fractions of minerals from andesites. The Mössbauer study was carried out by V.S. Rusakov at the Physical Department of Moscow State University at room temperature in absorption geometry in the mode of constant accelerations on an MS1101E spectrometer. The γ-quantum source was ^{57}Co on an Rh matrix. The results indicate that Fe^{3+} *per se* in the hornblende accounts for approximately 39%, and the isomer shifts for both Fe^{2+} and Fe^{3+} definitely indicate that both ion types are octahedrally coordinated.

Another important output of the research is the conclusion that roughly 14% Fe occurs in the fraction as a magnetically ordered phase, most probably magnetite (in spite of the fact that the use of a magnetic separator during sample preparation reduced to a minimum the possibility of the occurrence of hornblende–magnetite aggregates). The presence of finely crystalline (perhaps, cotectic) magnetite in the amphibole is generally consistent with the occurrence of larger inclusions of this mineral in the hornblendes inspected previously on a microprobe. Evidently, this fact should be taken into account when "bulk" hornblende analyses obtained by "wet chemistry" are interpreted.

The hornblendes had an average Fe^{3+}/Fe_{tot} ratio of 0.66 when calculated by the 13eCNK scheme, and the Fe^{3+} concentration estimated as an average between the minimum and maximum values [40] equals 0.41 (Fig. 5). This value is close to $Fe^{3+}/Fe_{tot} = 0.39$ yielded by Mössbauer spectroscopy, because of which we used the latter normalization scheme in the further calculation of the structural formulas of natural hornblendes (Table 2), including additional amphibole analyses compiled from the literature.

SUBSTITUTION TYPES IN HORNBLENDE FROM ANDESITES OF BEZYMYANNYI VOLCANO

In compliance with the IMA nomenclature proposed in 1997 [29], our hornblendes were classed with pargasite, magnesian hornblende, and tschermakite (Fig. 6). About 20% of them are high in Ti ($0.25 < Ti < 0.5$). In the classification diagrams, these compositions lie within a relatively compact field in which the Mg mole fraction varies insignificantly compared with the $^{[T]}Si$ and $^{[A]}Na + K$ variations.

In addition to simple isovalent substitutions ($Fe^{2+} \Leftrightarrow Mg^{2+}$ and $^{[A]}K \Leftrightarrow {}^{[A]}Na$), the compositional variability of amphiboles is commonly expressed in terms of exchange reactions with cations of different valences in the idealized tremolite formula, $\square Ca_2Mg_5Si_8O_{22}(OH)_2$. Extreme heterovalent substitutions result in other end members, whose names are used to designate a given cation exchange scheme (Table 3).

In the case of Ca-amphiboles, the most frequently discussed compositional vectors are edenitic, tschermakitic, pargasitic, and hastingsitic. Since these amphiboles contain more than 1.5 Ca f.u., the glaucophanic, riebeckitic, and richteritic exchange schemes (substitution of Ca for Na in [M4]) are of subordinate importance. This is readily seen in Fig. 7, which illustrates the possible substitution mechanisms in natural hornblendes in comparison with the field of experimentally synthesized Ca-amphiboles. In an $^{[A]}(Na + K)$ vs. $^{[4]}Al$ plot (Fig. 7a), the compositions of hornblende from the Bezymyannyi andesites define a trend parallel to a line connecting the pargasitic and hastingsitic substitutions, which are combinations of the edenitic (Fig. 7b) and tschermakitic (Fig. 7c) types. The intersection between the trend of naturally occurring amphiboles with the $^{[4]}Al \approx 0.7$ axis indicates that alkalis in [A] are compensated by $^{[4]}Al$, whose remaining part is related to octahedrally coordinated cations (Al, Fe^{3+}, and Ti), i.e., tschermakitic substitution. It should be mentioned that in $^{[4]}Al$ vs. Fe^{3+}, $^{[4]}Al$ vs. Ti, and $^{[4]}Al$ vs. $^{[6]}Al$ plots (Figs. 7d, 7e, 7f), the hornblende compositions do not define any clear-cut dependences, which suggests that there are simultaneously all tschermakitic types of substitution. The occurrence of tschermakitic substitutions is clearly demonstrated by the more complicated exchange type $^{[4]}Si + {}^{[6]}R^{2+} \Leftrightarrow {}^{[4]}Al + {}^{[6]}I$, where R is (Fe + Mg), and I is Al, Fe, and Ti (Fig. 7c offers an example of the Al-*Tsch* substitution). The dominant role of the edenitic and tschermakitic substitution types

Table 2. Exemplary calculation of a hornblende structural formula by three distinct procedures

Hbl analysis		Site	Cation	Normalization procedure		
				$Fe^3 = 0$	"average"	13eCNK
		[T]	Si	6.46	6.41	6.36
SiO_2	43.56		$^{[4]}Al$	1.54	1.59	1.64
TiO_2	2.00		$^{[6]}Al$	0.45	0.38	0.32
Al_2O_3	11.36		Ti	0.22	0.22	0.22
Fe_2O_3	0.00		Cr	0.00	0.00	0.00
FeO	14.57	$^{[M2]}C$	Fe^{3+}	0.00	0.39	0.70
MnO	0.17		Mn	0.02	0.02	0.02
MgO	12.20		Mg	0.55	0.46	0.38
CaO	11.06		Fe^{2+}	0.75	0.52	0.36
Na_2O	1.87	$^{[M1–3]}C$	Mg	2.13	2.22	2.27
K_2O	1.00		Fe^{2+}	0.87	0.78	0.73
			Mg	0.02	0.00	0.00
Total	97.79	$^{[M4]}B$	Fe^{2+}	0.18	0.10	0.00
			Ca	1.76	1.74	1.73
			Na	0.04	0.16	0.27
		A	Ca	0.00	0.00	0.00
			Na	0.50	0.38	0.26
			K	0.19	0.19	0.19
			□	0.32	0.43	0.55
			F	0.00	0.00	0.00
			Cl	0.00	0.00	0.00
			OH	2.00	2.00	2.00

is confirmed, first, by the absences of correlations between $^{[6]}Al$, Fe^{3+}, and $^{[A]}(Na + K)$ with Na in [M4] through the glaucophanic, edenitic, and richteritic substitutions, respectively (Figs. 7g–7i), and, second, by the linear dependence, with a slope equal to one, between tetrahedrally coordinated Al and the sum of $^{[A]}(Na + K) + 2Ti + Fe^{3+} + {}^{[6]}Al$ (Fig. 7j). The deviation of the trend from the 1 : 1 line in Fig. 7j suggests that the tschermakitic substitution may be coupled with a substitution of the glaucophanic type $2^{[M4]}Ca + {}^{[6]}Mg = 2^{[M4]}Na + Ti$ (Fig. 7k) [31, 48, 54]. Figure 7l illustrates a correlation between Fe and Mg, which is typical of the amphiboles.

THERMOBAROMETRY OF HORNBLENDES

The analyses of relations between substitutions of different types in hornblendes is necessitated by the fact that these substitutions are determined by variations in the intensive parameters during exchange reactions (in the case of metamorphic amphiboles) or crystallization processes (when magmatic amphiboles are considered). In particular, a substitution according to the tschermakitic scheme with the participation of $^{[M2]}Mg^{2+}$ and tetrahedrally coordinated Al^{3+} is sensitive to variations in the total pressure [12, 32] (Table 3). This tendency of the substitution of octahedrally coordinated (Mg, Fe) by Al was employed in a series of geobarometers, which are based on empirical observations and independent pressure estimates [31, 65] [Table 4, Eqs. (1)–(2)] or experimental data [32, 57] [Table 4, Eqs. (3)–(4)]. Equation (3) was calibrated with the use of higher temperature (720–780°C) experiments with rhyodacitic melts in the presence of a CO_2–H_2O fluid and pressures over the interval of 2–8 kbar [32]. Equation (4) was derived from the results of experiments with tonalite (58.95% SiO_2, 16.80% Al_2O_3, and 3.15% MgO) and granodiorite (66.66% SiO_2, 15.92% Al_2O_3, and 1.58% MgO), which were carried out within the near-solidus region (655–700°C) under pressures of 2.5–13 kbar [57].

It should be noted that Eqs. (1)–(4) in Table 4 were calibrated for the mineral assemblage *Qtz* + *Pl* + *Or* + *Hbl* + *Bi* + *Sph* + *Mt*(*Ilm*) in the subsolidus region of calk–alkaline granitoids and volcanic rocks, thus

Table 3. Main types of heterovalent substitutions in amphiboles on the bases of the idealized tremolite formula $\square Ca_2Mg_5Si_8O_{22}(OH)_2$

Substitution mechanism	End member	
$^{[A]}\square + {}^{[4]}Si = {}^{[A]}Na + {}^{[4]}Al$	Edenite	$NaCa_2Mg_5Si_7AlO_{22}(OH)_2$
$2^{[4]}Si + 2^{[6]}Mg = 2^{[4]}Al + 2^{[6]}Al$	Al-Tschermakite	$\square Ca_2(Mg_3Al_2)Si_6Al_2O_{22}(OH)_2$
$2^{[4]}Si + 2^{[6]}Mg = 2^{[4]}Al + 2^{[6]}Fe^{3+}$	Fe-Tschermakite	$\square Ca_2(Mg_3Fe^{3+}_2)Si_6Al_2O_{22}(OH)$
$2^{[4]}Si + {}^{[6]}Mg = 2^{[4]}Al + {}^{[6]}Ti$	Ti-Tschermakite	$\square Ca_2(Mg_4Ti)Si_6Al_2O_{22}(OH)_2$
$^{[A]}\square + {}^{[M4]}Ca = {}^{[A]}Na + {}^{[M4]}Na$	Richterite	$Na(CaNa)Mg_5Si_8O_{22}(OH)_2$
$2^{[M4]}Ca + 2^{[6]}Mg = 2^{[M4]}Na + 2^{[6]}Fe^{3+}$	Riebeckite	$\square Na_2(Fe^{2+}_3Fe^{3+}_2)Si_8O_{22}(OH)_2$
$2^{[M4]}Ca + 2^{[6]}Mg = 2^{[M4]}Na + 2^{[6]}Al$	Glaucophane	$\square Na_2(Mg_3Al_2)Si_8O_{22}(OH)_2$
$^{[A]}\square + {}^{[6]}Mg + 2^{[4]}Si = {}^{[A]}Na + 2^{[4]}Al + {}^{[6]}Al$	Hastingsite	$NaCa_2(Fe^{2+}_4Fe^{3+})Si_6Al_2O_{22}(OH)_2$
$^{[A]}\square + {}^{[6]}Mg + 2^{[4]}Si = {}^{[A]}Na + 2^{[4]}Al + {}^{[6]}Fe^{3+}$	Pargasite	$NaCa_2(Mg_4Al)Si_6Al_2O_{22}(OH)_2$

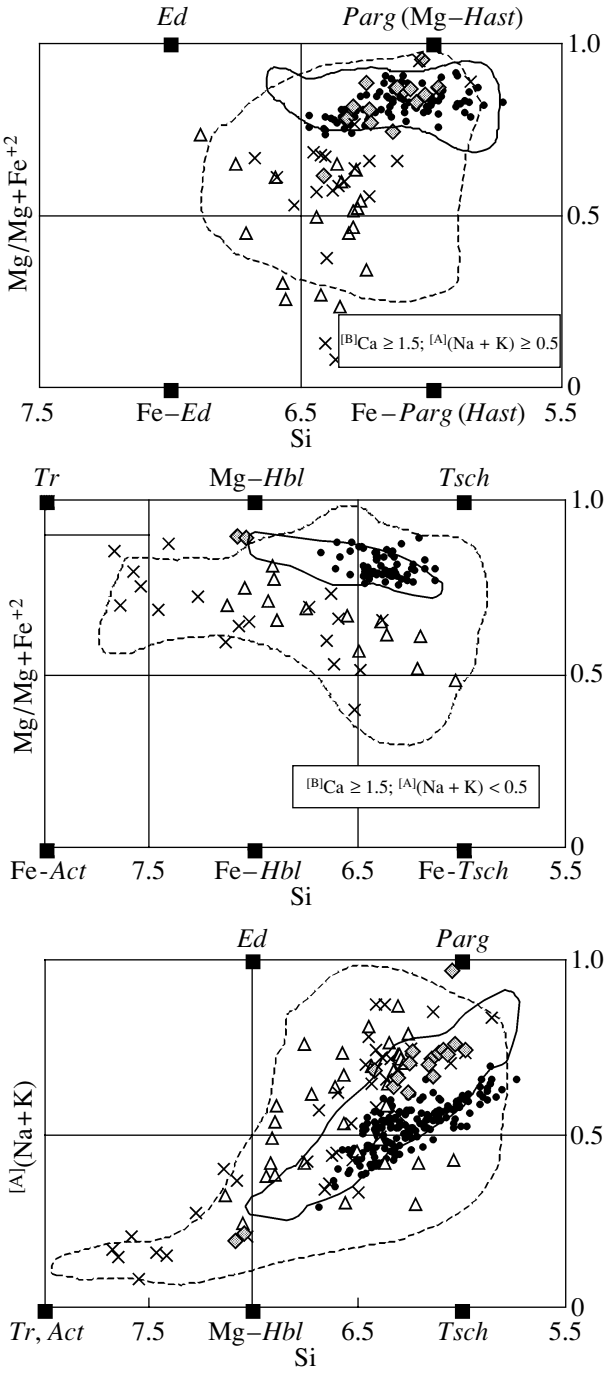

Fig. 6. Classification diagrams for hornblendes from andesites of Bezymyannyi volcano (symbols are the same as in Fig. 4).

implying that Al_{tot} in amphibole is sensitive to temperature. This limits the applicability of the empirical equations to only quartz-bearing assemblages, because, at the same *P–T* conditions, hornblendes crystallizing from melts with a lower SiO_2 activity and a higher Al_2O_3 activity are higher in alumina [32]. Because of this, the employment of these geobarometers in analyzing quartz-free assemblages (for example, basaltic andesites) should result in pressure overestimates.

In fact, the variations in Al_{tot} in amphiboles are not always caused by pressure variations. For example, it was established in experiments on the melting of naturally occurring (quartz-free) amphibolites that Al_{tot} in the synthesized hornblendes was independent of the variations in the total pressure within the range of 8–27 kbar [22]. It is known that Al is prone to replace tetrahedrally coordinated Si with an increase in temperature [12, 45, 54, 55, 66]. The temperature effect can explain some differences between pressure estimates relying on "experimental" barometers [32, 57]. A 100°C error in an estimate of a hornblende crystallization temperature leads to a pressure error of about 2 kbar [55], because of which Anderson proposed to utilize an expression relating pressure to temperature and Al_{tot} [Table 4, Eq. (5)].

On inspecting the chemistry of natural and synthetic Ca-amphiboles, Blundy and Holland [36, 46] questioned the conclusion of the predominant temperature dependence of the $^{[4]}Al$ and Al_{tot} contents. They explained variations in the alumina concentrations by means of the edenitic exchange scheme ($^{[A]}Na(K)^{[4]}Al \Leftrightarrow {}^{[A]}VAC^{[4]}Si$) in reactions participated by hornblende and plagioclase [Table 4, Eqs. (7)–(8)]. Already the very first versions of these geothermometers [46] found wide usage in the geothermometry of the *Hbl–Pl* assemblage, although they yielded overestimated temperatures for aluminous hornblendes. Also, the aforementioned researchers were criticized for underestimating the role of the tschermakitic substitution and for the use of an inadequate activity model for the components of hornblende [67, 68]. For example, it was demonstrated that variations in $^{[4]}Al$ in amphibole actually reflect an integral result of *Tsch*, *Ed*, and *Pl* substitutions [67], and the $^{[4]}Al$ concentration is sensitive not only to temperature but also to the activity of SiO_2 [68]. A temperature dependence was also identified in the distribution of alkaline cations (as components of the edenitic exchange): Helz reported [33] a temperature function for the Na and K exchange equilibrium between the [A] site in hornblende and melt [Table 4, Eq. (6)].

Hence, since natural hornblendes from the Bezymyannyi andesites exhibit both edenitic and tschermakitic substitutions (Figs. 7b, 7c), it can be theorized that their compositional variability was controlled by both temperature and pressure. At the same time, it is quite difficult to identify the purely baric dependence and assay the interval of pressures during hornblende crystallization. First, hornblende compositions do not define clear-cut trends in Figs. 7d, 7e, and 7f, as was observed in the case of genetically related Ca-amphiboles that crystallized under different pressures [31, 54, 55, 65]. Second, hornblendes that crystallize from melts with relatively low SiO_2 activities (no phenocrystic quartz is present) are high in Al_{tot} [32], which should result in pressure overestimates. This fact should be taken into account in interpreting barometric data on hornblende from andesites of Bezymyannyi volcano, for which a

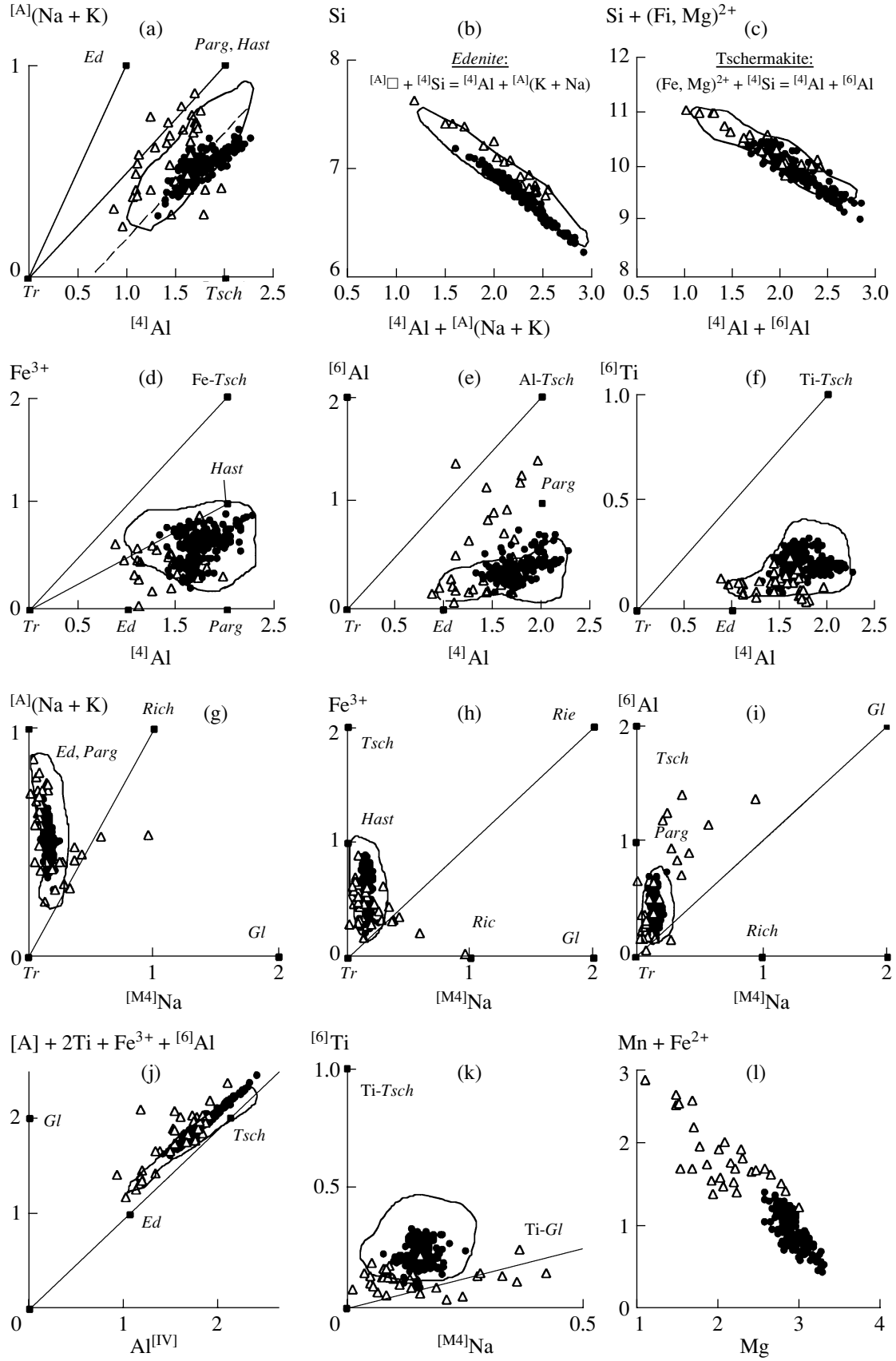

Fig. 7. Substitution mechanisms in hornblendes from andesites of Bezymyannyi volcano (see text).

Table 4. Hornblende geothermobarometry

	Geobarometers based on the Al concentration in hornblende
1	P (±3 kbar) = –3.92 + 5.03 Al_{tot}, r^2 = 0.80
2	P (±1 kbar) = –4.76 + 5.64 Al_{tot}, r^2 = 0.97
3	P (±0.5 kbar) = –3.46 + 4.23 Al_{tot}, r^2 = 0.99
4	P (±0.6 kbar) = –3.01 + 4.76 Al_{tot}, r^2 = 0.99
5	P (±0.6 kbar) = 4.76 Al_{tot} – 3.01{[T(°C) – 675]/85} × {0.530Al_{tot} + 0.005294[T(°C) – 675]}, r^2 = 0.99
	Temperature function of alkaline-cation distribution between melt and hornblende
6	$\ln \dfrac{X_K^{[A]} \cdot X_{Na}^{Liq}}{X_{Na}^{[A]} \cdot X_K^{Liq}} = 3.25 - \dfrac{4258}{T}$
	Hornblende–plagioclase geothermometers
7	(1) For the reaction *Ed* + 4 *Qtz* = *Tr* + *Ab*
	$T = \dfrac{-76.95 + 0.79P + Y_{Ab} + 39.4X_{Na}^{[A]} + 22.4X_K^{[A]} + (41.5 - 2.89P)X_{Al}^{[M2]}}{-0.0650 - R\ln\left(\dfrac{27X_{vac}^{[A]}X_{Si}^{[T1]}X_{Ab}^{Pl}}{256X_{Na}^{[A]}X_{Al}^{[T1]}}\right)}$
	for $X_{Ab}^{Pl} > 0.5 : Y_{Ab} = 0$
	for $X_{Ab}^{Pl} \le 0.5 : Y_{Ab} = 12(1 - X_{Ab}^{Pl})^2 - 3$
8	(2) For the reaction *Ed* + *Ab* = *Richt* + *An*
	$T = \dfrac{78.44 + Y_{Ab-An} - 33.6X_{Na}^{[M4]} - (66.8 - 2.92P)X_{Al}^{[M2]} + 78.5X_{Al}^{[T1]} + 9.4X_{Na}^{[A]}}{0.0721 - R\ln\left(\dfrac{27X_{Na}^{[M4]}X_{Si}^{[T1]}X_{Ab}^{Pl}}{64X_{Ca}^{[M4]}X_{Al}^{[T1]}X_{Ab}^{Pl}}\right)}$
	for $X_{Ab}^{Pl} > 0.5 : Y_{Ab-An} = 3$
	for $X_{Ab}^{Pl} \le 0.5 : Y_{Ab-An} = 12(2X_{Ab}^{Pl} - 1)^2 + 3$

Note: 1—[31]; 2—[65]; 3—[32]; 4—[57]; 5—[55]; 6—[33]; 7, 8—[36].

fairly broad interval of pressures was obtained [from 5 to 11 kbar (Fig. 8)], on the basis of a barometric diagram (Fig. 2b in [55] that disregards the temperature effect. The average Al_{tot} concentration in hornblendes (2.14 ± 0.27) points to dominant pressures of 6–8 kbar (Fig. 8), which presents a maximum estimate and is generally consistent with experimental data on amphibole stability in andesites from Bezymyannyi volcano [13, 69]. This conclusion is compatible with the concept of the fractionation of the water-bearing parental high-Al magmas at depths of less than 20 km [69].

If the pressure is known, the crystallization temperature can be estimated by the *Hbl–Pl* geothermometer [36] with the use of data on inclusions of these minerals in each other. Pairs of compositions for the systems inclusion–host mineral should represent a cotectic crystallization at a given temperature, and a series of these compositions for different crystals should characterize a certain temperature interval and fractionation stages. We examined the compositions of more than 20 plagioclase inclusions in hornblende from andesites of the 1956 eruption. No hornblende inclusions were detected in plagioclase phenocrysts from these rocks. Table 5 lists ten representative pairs of analyses and the corresponding estimates of the crystallization temperatures for the possible pressure interval of 6–8 kbar. The calculations were carried out by Eq. (8) (Table 4), which was calibrated for the *Ed* + *Ab* = *Richt* + *An* exchange equilibrium and can be applied to quartz-free assemblages. The estimated temperatures fall in the range 800–920°C.

CONCLUSIONS

This paper presents a review of the problem of estimating the Fe^{3+}/Fe_{tot} of naturally occurring and experimentally synthesized Ca-amphiboles. It is demonstrated that the currently utilized normalization

Table 5. Temperatures calculated based on analyses of plagioclase inclusions in hornblende

Grain	2–1		5–2		26		35		34		33		41–1		52–2		53–1		55	
	Hbl	*Plag*	*Hbl*	*Plag*	*Hbl*	*Plag*	*Hbl*	*Plag*	*Hbl*	*Plag*	*Hbl*	*Plag*	*Hbl*	*Plag*	*Hbl*	*Plag*	*Hbl*	*Plag*	*Hbl*	*Plag*
SiO_2	43.56	54.49	43.66	52.59	43.85	55.82	42.12	59.07	44.39	56.78	43.02	52.00	41.88	54.36	43.54	54.52	43.44	53.64	43.11	52.20
TiO_2	2.00		2.48		1.82		1.80		1.69		2.47		1.81		2.78		2.52		1.87	
Al_2O_3	11.36	28.72	11.18	29.90	12.11	27.48	12.63	24.32	10.98	25.27	12.10	30.78	15.20	29.04	12.49	29.41	12.10	30.15	12.19	31.67
FeO	14.57	0.60	13.99	0.39	13.77	0.59	13.87	0.85	14.37	1.05	14.17	0.42	12.71	0.39	12.80	0.44	14.43	0.31	14.98	0.39
MnO	0.17		0.30		0.31		0.29		0.35		0.24		0.22		0.24		0.19		0.32	
MgO	12.20	0.10	12.99	0.04	12.71	0.09	12.93	0.15	12.82	0.22	13.12	0.05	12.94	0.03	12.92	0.07	13.14	0.02	12.14	0.03
CaO	11.06	10.68	11.09	12.20	11.11	9.36	11.43	6.52	10.86	7.51	11.25	13.13	11.45	11.08	11.25	11.37	11.23	12.15	10.87	13.92
Na_2O	1.87	5.14	2.17	4.22	2.08	5.75	2.21	6.56	1.76	5.99	1.99	3.76	2.26	4.83	2.12	4.80	2.12	4.22	1.89	3.83
K_2O	1.00	0.21	0.58	0.17	0.47	0.26	0.76	1.38	0.53	1.55	0.51	0.13	0.50	0.18	0.60	0.20	0.69	0.15	0.61	0.14
Cr_2O_3	0.04		0.00		0.04		0.00		0.03		0.00		0.04		0.00		0.07		0.07	
Σ	97.83	99.93	97.21	99.50	98.27	99.34	98.04	98.85	97.78	98.37	98.86	100.27	99.0	99.90	98.74	100.80	99.94	100.64	98.05	102.17
An, mol %		52.76		60.89		46.65		32.54		37.18		65.38		55.33		56.06		60.68		66.22
$\frac{Mg}{Mg+Fe^{2+}}$	0.66		0.70		0.70		0.72		0.70		0.73		0.74		0.70		0.70		0.68	
Temperature values calculated for the *Ed* + *Ab* = *Richt* + *An* exchange equilibrium [Table 4, Eq. (8)] for pressures of 6, 8, and 10 kbar																				
6 kbar	843		899		821		816		799		909		838		857		908		874	
8 kbar	854		907		834		824		809		917		854		869		916		887	
10 kbar	865		915		847		833		820		925		871		882		924		899	

Note: The calculations were carried out by the HbPlag computer program (http://www.esc.cam.ac.uk/astaff/holland/hbplag.html).

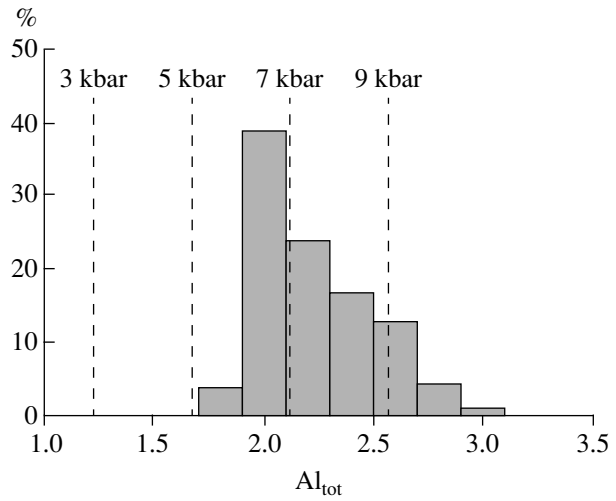

Fig. 8. Histogram of the distribution of Al_{tot} values of the hornblendes of Bezymyannyi volcano. Isobaric sections are according to [55].

schemes of chemical analyses cannot yield satisfactory results, because all procedures underestimate Fe_2O_3 and overestimate FeO. For hornblendes from the calc–alkaline lavas of Bezymyannyi volcano, we used the method of "an average between the maximum and minimum Fe^{3+} estimates," because the average values (39% Fe^{3+}) are close to the Mössbauer data. The calculated structural formulas of the amphiboles imply the edenitic and tschermakitic mechanisms of heterovalent substitutions. This led us to suggest that their compositions evolved during the fractionation of a cooling andesitic melt at a relatively insignificant pressure decrease.

The currently existing geothermometers were designed for estimating intensive parameters on the basis of cation concentrations at certain structural sites or through cation exchange in the crystal structure. Other approaches are based on complex exchange equilibria between solid phases. The only temperature equation [33] proposed to account for relations between the Na/K ratio of amphibole and melt in melt–mineral equilibria is still not widely used. This led us to conclude that the use of magmatic amphiboles for geothermobarometric purposes is generally problematic due to the complexity of the chemistry of this mineral, analytical uncertainties, and the probable lack of equilibrium between the minerals.

This situation explains the absence of any more or less consistent models for amphibole–melt equilibria, which could be used in the computer simulation of the crystallization of water-bearing andesitic magmas. We believe that the study of the effect of hornblende crystallization on natural trends can be provisionally simplified if models for Ca-amphibole crystallization are developed by limiting the consideration to a certain "bulk hornblende component" in compliance with the specified P–T–f_{O_2}–a_{H_2O} parameters. A possible solution to this problem is to design a system of semiempirical equations relating the hornblende–melt partition coefficients for all components and the mass-balance conditions over all solid phases, as was proposed in [70].

ACKNOWLEDGMENTS

The authors thank V.S. Rusakov and A.M. Bychkov for help in the Mössbauer study. The authors are indebted to K. Currie, who provided the initial code and calculation program of Fe^{2+} in amphibole. We also thank S.A. Silant'ev for constructive comments on the manuscript. This study was supported by the Russian Foundation for Basic Research, project nos. 99-05-64875 and 00-05-64466 and a grant of the 6th Competition–Expertise of Young Researchers of the Russian Academy of Sciences.

REFERENCES

1. Bowen, N.L., The Reaction Principle in Petrogenesis, *J. Geol.*, 1922, vol. 30, pp. 177–198.
2. Tilley, C.E., Some Aspects of Magmatic Evolution, *Geol. Soc. London Quart. J.*, 1950, vol. 106, pp. 37–61.
3. Boyd, F.R., Hydrothermal Investigation of Amphiboles, in *Researches in Geochemistry*, New York: Wiley, 1959, pp. 377–396.
4. Yoder, H.S., Calc-Alkaline Andesites: Experimental Data Bearing on the Origin of Their Assumed Characteristics, in *Proceedings of the Andesites*, Oregon: Dept. Geol., 1969, pp. 77–89.
5. Takeshita, H., Petrological Studies on the Volcanic Rocks of the Northern Fossa Magma Region, Central Japan, *Pacific Geol.*, 1974, vol. 7, pp. 65–92.
6. Cawthom, R.G., Curran, E.B., and Arculus, R.J., A Petrogenetic Model for the Origin of the Calc-Alkaline Suite of Grenada, Lesser Antilles, *J. Petrol.*, 1973, vol. 14, pp. 327–337.
7. Cawthom, R.G. and O'Hara, M.J., Amphibole Fractionation in Calc-Alkaline Magma Genesis, *Am. J. Sci.*, 1976, vol. 276, no. 3, pp. 309–329.
8. Devine, J.D. and Sigurdsson, H., Petrology and Eruption Styles of Kick'Em-Jenny Submarine Volcano, Lesser Antilles Island Arc, *J. Volcanol. Geotherm. Res.*, 1995, vol. 69, nos. 1–2, pp. 35–58.
9. Thirlwall, M.F., Graham, A.M., Arculus, R.J., *et al.*, Resolution of the Effects of Crustal Assimilation, Sediment Subduction, and Fluid Transport in Island Arc Magmas: Pb–Sr–Nd–O Isotope Geochemistry of Grenada, Lesser Antilles, *Geochim. Cosmochim. Acta*, 1996, vol. 60, no. 23, pp. 4785–4810.
10. Best, M.C. and Wercey, E.L.P., Composition and Crystallization of Mafic Minerals in the Guadalupe Igneous Complex, California, *Am. Mineral.*, 1967, vol. 52, pp. 436–474.
11. Yoder, H.S. and Tilley, C.E., Origin of Basaltic Magma: An Experimental Study of Natural and Synthetic Rock Systems, *J. Petrol.*, 1962, vol. 3, pp. 342–532.
12. Helz, R.T., Phase Relations and Compositions of Amphiboles Produced in Studies of the Melting Behavior of Rocks, in *Amphiboles: Petrology and Experimen-*

tal Phase Relations, Washington: Mineral. Soc. Am., 1982, vol. 9B, pp. 279–353.

13. Kadik, A.A., Maksimov, A.P., and Ivanov, B.V., *Fiziko-khimicheskie usloviya kristallizatsii i genezis andezitov (na primere Klyuchevskoi gruppy vulkanov)* (Andesites of the Klyuchevskaya Group of Volcanoes: The Physicochemical Conditions of Crystallization and the Genesis), Moscow: Nauka, 1986.
14. Hilyard, M., Niefsen, R.L., Beard, J.S., *et al.*, Experimental Determination of the Partitioning Behavior of Rare Earth and High Field Strength Elements between Pargasitic Amphibole and Natural Silicate Melts, *Geochim. Cosmochim. Acta*, 2000, vol. 64, no. 6, pp. 1103–1120.
15. Romick, J.D., Kay, S.M., and Kay, R.W., The Influence of Amphibole Fractionation on the Evolution of Calc-Alkaline Andesite and Dacite Tephra from the Central Aleutians, Alaska, *Contrib. Mineral. Petrol.*, 1992, vol. 112, no. 1, pp. 101–118.
16. Hunter, A.G., Intracrustal Controls on the Coexistence of Tholeiitic and Calc-Alkaline Magma Series of Aso Volcano, SW Japan, *J. Petrol.*, 1998, vol. 39, no. 7, pp. 1255–1284.
17. Kimura, J.I. and Yoshida, T., Magma Plumbing System beneath Ontake Volcano, Central Japan, *The Island Arc*, 1999, vol. 8, pp. 1–29.
18. Foden, J., The Petrology of Calc-Alkaline Lavas of Rindjani Volcano, East Sunda Arc: A Model for Island Arc Petrogenesis, *J. Petrol.*, 1983, vol. 24, pp. 98–130.
19. Arculus, R.J., Aspects of Magma Genesis in Arcs, *Lithos*, 1994, vol. 33, pp. 189–208.
20. Ariskin, A.A. and Barmina, G.S., *Modelirovanie fazovykh ravnovesii pri kristallizatsii bazal'tovykh magm* (Modeling the Phase Equilibria in Crystallization of Basaltic Magmas), Moscow: Nauka, 2000.
21. Tatsumi, Y. and Eggins, S., *Subduction Zone Magmatism*, Cambridge: Blackwell, 1995.
22. Rapp, R.P. and Watson, E.B., Dehydration Melting of Metabasalt at 8–32 Kbar: Implications for Continental Growth and Crust–Mantle Recycling, *J. Petrol.*, 1995, vol. 36, no. 4, pp. 891–931.
23. Ariskin, A.A., Meshalkin, S.S., Al'meev, R.R., *et al.*, INFOREX Information Retrieval System: Analysis and Processing of Experimental Data on Phase Equilibria in Igneous Rocks, *Petrologiya*, 1997, vol. 5, no. 1, pp. 32–41.
24. Hawthorne, F.C., The Crystal Chemistry of the Amphiboles, *Can. Mineral.*, 1983, vol. 21, pp. 173–480.
25. King, P.L., Hervig, R.L., Holloway, J.R., *et al.*, Partitioning of Fe^{3+}/Fe_{tot} between Amphibole and Basanitic Melt as a Function of Oxygen Fugacity, *Earth Planet. Sci. Lett.*, 2000, vol. 178, nos. 1–2, pp. 97–112.
26. Cosca, M.A., Essence, E.J., and Bowman, J.R., Complete Chemical Analyses of Metamorphic Hornblendes: Implications for Normalizations, Calculated H_2O Activities, and Thermobarometry, *Contrib. Mineral. Petrol.*, 1991, vol. 108, pp. 472–484.
27. Scaillet, B. and Evans, B.W., The 15 June 1991 Eruption of Mount Pinatubo. 1. Phase Equilibria and Pre-Eruption $T–f_{O_2}–f_{H_2O}$ Conditions of the Dacite Magma, *J. Petrol.*, 1999, vol. 40, no. 3, pp. 381–411.
28. Klimm, K., Johannes, W., and Koepke, J., Dehydration Melting Reaction of Amphibole: A Comparative Study of Melting and Crystallization Experiments, *EMPG VIII*, Italy, Bergamo, 2000, p. 58.
29. Leake, B.E. *et al.*, Nomenclature of Amphiboles: Report of the Subcommittee on Amphiboles of the International Mineralogical Association, Comission on New Minerals and Mineral Names, *Can. Mineral.*, 1997, vol. 35, no. 1, pp. 219–246.
30. Graham, C.M. and Navrotsky, A., Thermochemistry of the Tremolite–Edenite Amphiboles Using Fluorine Analogues, and Applications to Amphibole–Plagioclase–Quartz Equilibria, *Contrib. Mineral. Petrol.*, 1986, vol. 93, no. 1, pp. 18–32.
31. Hammarstrom, J.M. and Zen. E.-A. Aluminum in Hornblende: An Empirical Igneous Geobarometer, *Am. Mineral.*, 1986, vol. 71, nos. 11–12, pp. 1297–1313.
32. Johnson, M.C. and Rutherford, M.J., Experimental Calibration of the Aluminum-in-Hornblende Geobarometer with Application to Long Valley Caldera (California) Volcanic Rocks, *Geology*, 1989, vol. 17, pp. 837–841.
33. Helz, R.T., Alkali Exchange between Hornblende and Melt: A Temperature-Sensitive Reaction, *Am. Mineral.*, 1979, vol. 64, nos. 9–10, pp. 953–965.
34. Ravna, E.K., Distribution of Fe^{2+} and Mg between Coexisting Garnet and Hornblende in Synthetic and Natural Systems: An Empirical Calibration of the Garnet–Hornblende Fe–Mg Geothermometer, *Lithos*, 2000, vol. 53, nos. 3–4, pp. 265–277.
35. Spear, F.S., Amphibole–Plagioclase Equilibria: An Empirical Model for the Relation Albite + Tremolite = Edenite + 4 Quartz, *Contrib. Mineral. Petrol.*, 1981, vol. 77, no. 4, pp. 355–364.
36. Holland, T. and Blundy, J., Non-Ideal Interactions in Calcic Amphiboles and Their Bearing on Amphibole–Plagioclase Thermometry, *Contrib. Mineral. Petrol.*, 1994, vol. 116, no. 4, pp. 433–447.
37. Dale, J., Holland, T.J.B., and Powell, R., Hornblende–Garnet–Plagioclase Thermobarometry: A Natural Assemblage Calibration of the Thermodynamics of Hornblende, *Contrib. Mineral. Petrol.*, 2000, vol. 140, no. 3, pp. 353–362.
38. Sack, R.O., Spinels as Petrogenetic Indicators: Activity-Composition Relations at Low Pressures, *Contrib. Mineral. Petrol.*, 1982, vol. 79, pp. 169–186.
39. Powell, R., Thermodynamics of Coexisting Cummingtonite–Hornblende Pairs, *Contrib. Mineral. Petrol.*, 1975, vol. 51, no. 1, pp. 29–37.
40. Schumacher, J.C., The Estimation of the Proportion of Ferric Iron in the Electron-Microprobe Analysis of Amphiboles, *Can. Mineral.*, 1997, vol. 35, no. 1, pp. 238–246.
41. Robinson, P., Spear, F.S., Schumacher, J.C., *et al.*, Phase Relations of Metamorphic Amphiboles: Natural Occurrence and Theory, in *Amphiboles: Petrology and Experimental Phase Relations*, Washington: Mineral. Soc. Am., 1982, vol. 9B, pp. 1–227.
42. Currie, K.L., A Revised Computer Program for Amphibole Classification, *Can. Mineral.*, 1997, vol. 35, no. 5, pp. 1351–1352.
43. Schumacher, J.C., Empirical Ferric Iron Corrections: Necessity, Assumptions, and Effects on Selected Geo-

thermobarometers, *Mineral. Mag.*, 1991, vol. 55, pp. 3–18.

44. Makino, K. and Tomita, K., Cation Distribution in the Octahedral Sites of Hornblendes, *Am. Mineral.*, 1989, vol. 74, nos. 9–10, pp. 1097–1105.
45. Ernst, W.G. and Liu, L., Experimental Phase-Equilibrium Study of Al- and Ti-Contents of Calcic Amphibole in MORB: A Semiquantitative Thermobarometer, *Am. Mineral.*, 1998, vol. 83, pp. 952–969.
46. Blundy, J.D. and Holland, J.B., Calcic Amphibole Equilibria and a New Amphibole–Plagioclase Geothermometer, *Contrib. Mineral. Petrol.*, 1990, vol. 104, no. 2, pp. 208–224.
47. Clowe, C.A., Popp, R.K., and Fritz, S.J., Experimental Investigation of the Effect of Oxygen Fugacity on Ferric–Ferrous Ratios and Unit-Cell Parameters in Four Natural Clinoamphiboles, *Am. Mineral.*, 1988, vol. 73, nos. 5–6, pp. 487–499.
48. Spear, F.S., An Experimental Study of Hornblende Stability and Compositional Variability in Amphibolite, *Am. J. Sci.*, 1981, vol. 281, no. 6, pp. 697–734.
49. Carmichael, I.S.E. and Ghiorso, M.S., The Effect of Oxygen Fugacity on the Redox State of Natural Liquids and Their Crystallizing Phases, in *Modern Methods of Igneous Petrology: Understanding Magmatic Processes*, Washington: Mineral. Soc. Am., 1990, vol. 24, pp. 192–210.
50. Ulmer, G.C., Rosenhauer, M., Woermann, E., *et al.*, Applicability of Electrochemical Oxygen Fugacity Measurements to Geothermometry, *Am. Mineral.*, 1976, vol. 61, pp. 653–660.
51. Popp, R.K., Virgo, D., Yoder, H.S., *et al.*, An Experimental Study of Phase Equilibria and Fe Oxy-Component in Kaersutitic Amphibole: Implications for the f_{H_2} and a_{H_2O} in the Upper Mantle, *Am. Mineral.*, 1995, vol. 80, pp. 534–548.
52. Delaney, J.S., Bajt, S., Sutton, S.R., and Dyar, M.D., *In situ* Microanalysis of Fe^{3+}/Fe in Amphibole by X-Ray Absorption Near Edge Structure (XANES) Spectroscopy, *Geochem. Soc. Spec. Publ.*, 1996, vol. 5: *Mineral Spectroscopy: A Tribute to Roger G. Burns*, pp. 165–171.
53. Nikolaev, G.S., Borisov, A.A., and Ariskin, A.A., Calculation of Ferric–Ferrous Ratio in Magmatic Melts: Testing and Additional Calibration of Empirical Equations for Various Magmatic Series, *Geokhimiya*, 1996, no. 8, pp. 713–722.
54. Vyhnal, C.R., McSween, H.Y., and Speer, J.A., Hornblende Chemistry in Southern Appalachian Granitoids: Implications for Aluminum Hornblende Thermobarometry and Magmatic Epidote Stability, *Am. Mineral.*, 1991, vol. 76, nos. 1–2, pp. 176–188.
55. Anderson, J.L. and Smith, D.R., The Effects of Temperature and f_{O_2} on the Al-in-Hornblende Barometer, *Am. Mineral.*, 1995, vol. 80, pp. 549–559.
56. Rutter, M.J., Van der Laan, S.R., and Wyllie, P.J., Experimental Data for a Proposed Empirical Igneous Geobarometer: Aluminum in Hornblende at 10 Kbar Pressure, *Geology*, 1989, vol. 17, pp. 897–900.
57. Schmidt, M.W., Amphibole Composition in Tonalite as a Function of Pressure: An Experimental Calibration of the Al-in-Hornblende Barometer, *Contrib. Mineral. Petrol.*, 1992, vol. 110, no. 2/3, pp. 304–310.
58. Sisson, T.W., Grove, T.L., and Coleman, D.S., Hornblende Gabbro Sill Complex at Onion Valley, California, and a Mixing Origin for the Sierra Nevada Batholith, *Contrib. Mineral. Petrol.*, 1996, vol. 126, nos. 1–2, pp. 81–108.
59. Meijer, A. and Reagan, M., Petrology and Geochemistry of the Island of Sarigan in the Mariana Arc: Calc-Alkaline Volcanism in an Oceanic Setting, *Contrib. Mineral. Petrol.*, 1981, vol. 77, pp. 337–354.
60. Hebert, R., Serri, G., and Hekinian, R., Mineral Chemistry of Ultramafic Tectonites and Ultramafic to Gabbroic Cumulates from the Major Oceanic Basins and Northern Apennine Ophiolites (Italy): A Comparison, *Chem. Geol.*, 1989, vol. 77, pp. 183–207.
61. Graham, C.M., Metabasite Amphiboles of the Scottish Dalradian, *Contrib. Mineral. Petrol.*, 1974, vol. 47, no. 3, pp. 165–185.
62. Lange, R.A. and Carmichael, I.S.E., The Aurora Volcanic Field, California–Nevada: Oxygen Fugacity Constraints on the Development of Andesitic Magma, *Contrib. Mineral. Petrol.*, 1996, vol. 125, no. 2/3, pp. 167–185.
63. Wones, D.R. and Gilbert, M.C., Amphiboles in the Igneous Environment, in *Amphiboles: Petrology and Experimental Phase Relations*, Washington: Mineral. Soc. Am., 1982, vol. 9B, pp. 355–390.
64. Al'meev R.R. and Rusakov, V.S., Mössbauer Studies of Amphibole in Andesites of the Bezymyannyi Volcano, Eastern Kamchatka, *Vestn. OGGGGN RAS*, 2000, vol. 1(5), no. 15, p. 23.
65. Hollister, L.S., Grissom, G.C., Peters, E.K., *et al.*, Confirmation of the Empirical Correlation of Al in Hornblende with Pressure of Solidification of Calc-Alkaline Plutons, *Am. Mineral.*, 1987, vol. 72, pp. 231–239.
66. Hawthorne, F.C., Crystal Chemistry of the Amphiboles, in *Amphiboles and Other Hydrous Pyriboles: Mineralogy*, Washington: Mineral. Soc. Am., 1981, vol. 9A, pp. 1–102.
67. Poli, S. and Schmidt, M.W., A Comment on "Calcic Amphibole Equilibria and a New Amphibole–Plagioclase Geothermometer" by J. D. Blundy and T. J. B. Holland (*Contrib. Mineral. Petrol.*, 1990, 104: 208–224), *Contrib. Mineral. Petrol.*, 1992, vol. 111, no. 2, pp. 273–278.
68. Rutherford, M.J. and Johnson, M.C., A Comment on Blundy and Holland's (1990) "Calcic Amphibole Equilibria and a New Amphibole–Plagioclase Geothermometer," *Contrib. Mineral. Petrol.*, 1992, vol. 111, no. 2, pp. 266–268.
69. Ozerov, A., Ariskin, A.A., Kail, F., *et al.*, Petrological–Geochemical Model for Genetic Relationships between Basaltic and Andesitic Magmatism of Klyuchevskoi and Bezymyannyi Volcanoes, Kamchatka, *Petrologiya*, 1997, vol. 5, no. 6, pp. 614–635.
70. Ariskin, A.A. and Barmina, G.S., An Empirical Model for the Calculation of Spinel–Melt Equilibria in Mafic Igneous Systems at Atmospheric Pressure: 2. Fe–Ti Oxides, *Contrib. Mineral. Petrol.*, 1999, vol. 134, pp. 241–263.